Macitentan reduces progression of TGF-β1-induced pulmonary fibrosis and pulmonary hypertension

Pierre-Simon Bellaye[1,2,5], Toyoshi Yanagihara[1,5], Elise Granton[1], Seidai Sato[1,3], Chiko Shimbori[1], Chandak Upagupta[1], Jewel Imani[1], Nathan Hambly[1], Kjetil Ask[1], Jack Gauldie[1], Marc Iglarz[4] and Martin Kolb[1]

Affiliations: [1]Firestone Institute for Respiratory Health, Research Institute at St Joseph's Healthcare, Dept of Medicine, McMaster University, Hamilton, ON, Canada. [2]Plateforme d'Imagerie et Radiothérapie Préclinique, Centre George-François Leclerc (CGFL), Dijon, France. [3]Dept of Respiratory Medicine and Rheumatology, Graduate School of Biomedical Sciences, Tokushima University, Tokushima, Japan. [4]Actelion Pharmaceuticals Ltd, Allschwil, Switzerland. [5]These authors contributed equally to this work.

Correspondence: Martin Kolb, Dept of Respiratory Medicine, Pathology and Molecular Medicine, McMaster University, 50 Charlton Avenue East, Hamilton, ON L8N 4A6, Canada. E-mail: kolbm@mcmaster.ca

@ERSpublications
Macitentan reduces the progression of TGF-β1-induced pulmonary fibrosis and pulmonary hypertension, while pirfenidone only slows fibrosis progression http://ow.ly/4tt230kHQOn

Cite this article as: Bellaye P-S, Yanagihara T, Granton E, *et al.* Macitentan reduces progression of TGF-β1-induced pulmonary fibrosis and pulmonary hypertension. *Eur Respir J* 2018; 52: 1701857 [https://doi.org/10.1183/13993003.01857-2017].

ABSTRACT Idiopathic pulmonary fibrosis (IPF) is a progressive disease with an unknown cause. Two drugs, nintedanib and pirfenidone, have been shown to slow, but not stop, disease progression. Pulmonary hypertension (PH) is a frequent complication in IPF patients and is associated with poor prognosis. Macitentan is a dual endothelin receptor antagonist that is approved for pulmonary arterial hypertension treatment. We hypothesised that using macitentan to treat animals with pulmonary fibrosis induced by adenoviral vector encoding biologically active transforming growth factor-β1 (AdTGF-β1) would improve the PH caused by chronic lung disease and would limit the progression of fibrosis.

Rats (Sprague Dawley) which received AdTGF-β1 were treated by daily gavage of macitentan (100 $mg \cdot kg^{-1} \cdot day^{-1}$), pirfenidone (0.5% food admix) or a combination from day 14 to day 28. Pulmonary artery pressure (PAP) was measured before the rats were killed, and fibrosis was subsequently evaluated by morphometric measurements and hydroxyproline analysis.

AdTGF-β1 induced pulmonary fibrosis associated with significant PH. Macitentan reduced the increase in PAP and both macitentan and pirfenidone stopped fibrosis progression from day 14 to day 28. Macitentan protected endothelial cells from myofibroblast differentiation and apoptosis whereas pirfenidone only protected against fibroblast-to-myofibroblast differentiation. Both drugs induced apoptosis of differentiated myofibroblasts *in vitro* and *in vivo*.

Our results demonstrate that dual endothelin receptor antagonism was effective in both PH and lung fibrosis whereas pirfenidone only affected fibrosis.

This article has supplementary material available from erj.ersjournals.com

Received: Sept 12 2017 | Accepted after revision: June 24 2018

Introduction

Idiopathic pulmonary fibrosis (IPF) is characterised by progressive lung tissue scarring and destruction of alveolar architecture. The prevalence of IPF is 20–42 per 100 000 in the general population and up to 245 per 100 000 in the age group >70 years. The prognosis of IPF is poor, with a mortality rate comparable to aggressive cancers. The precise cause of IPF remains elusive and treatment options are limited to only two approved drugs, nintedanib and pirfenidone, which have been shown to slow progression but not stop the disease [1–3]. The pathogenesis of IPF is viewed as aberrant and involves uncontrolled alveolar repair, in which the differentiation and persistence of myofibroblasts represents a crucial event. Myofibroblasts clustered in fibroblastic foci are responsible for the abnormal accumulation of extracellular matrix (ECM). Transforming growth factor-β1 (TGF-β1) plays a key role in IPF by inducing myofibroblast differentiation [4].

Pulmonary hypertension (PH) is a recognised complication of IPF and a marker of poor prognosis [5]. PH is characterised by a persistent increase in mean pulmonary arterial pressure (PAP) >25 mmHg [6]. Histologically, PH presents with endothelial cell (EC) injury and vascular smooth muscle cell (VSMC) proliferation. Endothelin-1 (ET-1) is a potent vasoconstrictor that binds to ETA and ETB receptors (ETRA and ETRB) present on pulmonary fibroblasts, VSMCs and ECs [7]. ET-1 is expressed in IPF lungs and in bleomycin-induced pulmonary fibrosis [8]. Moreover, ET-1 favours myofibroblast differentiation, persistence and resistance to apoptosis [9]. Our group demonstrated that the adenovector-mediated gene transfer of active TGF-β1 (AdTGF-β1) in rodent lungs leads to progressive and severe fibrosis coupled with PH through decreased expression of vascular endothelial growth factor (VEGF), enhanced EC apoptosis, subsequent vascular rarefaction and TGF-β1-driven media thickening [10]. Macitentan is a dual ETRA/ETRB antagonist approved for the treatment of pulmonary arterial hypertension (PAH) [6]. In the bleomycin rat model of lung fibrosis, macitentan demonstrated efficacy in reducing right ventricle hypertrophy and pulmonary remodelling [11]. Despite promising preclinical data, the Macitentan USe in IPF Clinical (MUSIC) trial failed to show benefits of the drug for IPF patients [12]. However, this trial was conducted in patients with mild to moderate IPF who probably did not (yet) have significant remodelling of the pulmonary vasculature and PH. Therefore, further studies are needed to understand the real impact of ET-1 blockers on advanced IPF.

We investigated the efficacy and mechanisms by which dual ET receptor antagonism affects lung fibrosis and PH induced by AdTGF-β1 in rats in comparison to pirfenidone. We demonstrate for the first time that macitentan, in addition to regressing TGF-β1-induced PH, inhibits the progression of TGF-β1-induced lung fibrosis in rats.

Materials and methods

See supplementary material for detailed methods.

Human samples

Plasma and tissue were collected with patients' consent and approval from the Hamilton Integrated Research Ethics Board (HIREB #00–1839). Control lung tissue was from patients undergoing a surgical procedure for cancer. Lung fibrosis tissue was from patients undergoing a biopsy for unclear interstitial lung disease. The biopsies analysed in this study revealed a usual interstitial pneumonia pattern.

Antibodies and reagents

Antibodies used were α-smooth muscle actin (α-SMA) (ab7817; Abcam, Cambridge, UK), pSmad3 (ab51451; Abcam), Smad3 (ab40854; Abcam), VEGF (ab1316; Abcam), cleaved caspase-3 (#9661; Cell Signaling Technology, Danvers, MA, USA), ET-1 (ab117757; Abcam), CD31 (sc-1506; Santa Cruz Biotechnology, Santa Cruz, CA, USA), ETRA (ab117521; Abcam), ETRB (ab117529; Abcam), GAPDH (#5174; Cell Signaling Technology), anti-rabbit HRP-linked IgG (#7074; Cell Signalling Technology) and anti-mouse IgG HRP-linked antibody (#7076; Cell Signaling Technology). For fluorescence microscopy, we used goat or donkey secondary antibody conjugated with Alexa Fluor-488 and Alexa Fluor-555 (Abcam). Human rET-1 (100-21; PerproTech, London, UK) and human rTGF-β1 (240-B; R&D Systems, Minneapolis, MN, USA) were used *in vitro* to treat cells.

Cell culture

Human-derived normal primary pulmonary artery smooth muscle cells (PCS-100-023; ATCC, Manassas, VA, USA) and primary pulmonary artery ECs (PCS-100-022; ATCC) were grown according to manufacturer's recommendations. Fibroblasts were obtained from humans during surgical biopsy (control and IPF) and grown in RPMI medium (30-2001; ATCC) supplemented with 10% fetal bovine serum. All cells were incubated at 37°C in 5% CO_2.

Animal experiments

Animal work was conducted under guidelines from the Canadian Council on Animal Care and approved by the Animal Research Ethics Board of McMaster University (#13-12-48). Pulmonary fibrosis was induced by AdTGF-β1. Female Sprague Dawley rats (225–250 g; Charles River Laboratories, Wilmington, MA, USA) received 5.0×10^8 plaque-forming units (PFU) of AdTGF-β1 by intratracheal instillation under isoflurane anaesthesia at day 0 (D0). Rats received macitentan (daily gavage 100 $mg\cdot kg^{-1}\cdot day^{-1}$; Actelion Pharmaceuticals Ltd., Allschwil, Switzerland), pirfenidone (0.5% food admix *ad libitum*; Chemcia Scientific, San Diego, CA, USA) or a combination of both (n=6 per group) from D14 to D28. Before they were killed, rats were anesthetised and a catheter (PE tubing, SP0109; ADInstruments Inc., Colorado Springs, CO, USA) was introduced into the jugular vein and pushed further into the pulmonary artery to read the PAP with a pressure transducer (MLT844; ADInstruments Inc.). Lungs were harvested *post mortem* and fixed in 10% formalin for histology or flash-frozen in liquid nitrogen for protein and RNA analysis.

Computed tomography scan imaging

See supplementary material for details.

Western blotting

See supplementary material for details.

Hydroxyproline assay

Hydroxyproline content in lung tissue was measured by a colorimetric assay as described previously [13]. See supplementary material for details.

Ashcroft score

Pulmonary fibrosis of Masson trichrome-stained lung sections was graded from 0 (normal) to 8 (completely fibrotic lung), using a modified Ashcroft score [14].

Isolation of mRNA and gene expression

Total RNA was extracted from frozen lung tissue with TRIzol® reagent (15596026; Thermo Fisher Scientific, Waltham, MA, USA). qScript cDNA SuperMix (95048-025; Quanta Bioscience, Gaithersburg, MD, USA) was used to reverse transcribe 2 µg of total RNA. The cDNA was amplified using a Fast 7500 real-time PCR system (Applied Biosystems, Foster City, CA, USA) using TaqMan® Universal PCR Master Mix and predesigned primer pairs (4304437; Life Technologies, Burlington, ON, Canada) for Collagen1A (Hs00164004_m1), TGFβR1 (Hs00610320_m1), ACTA2 (Hs00426835_g1) and 18S (Hs03003631_g1).

Histology and immunohistochemistry

Lung slides were stained with Masson trichrome or Picrosirius red. Picture acquisition was performed using an automatic slide scanner microscope (Olympus VS 120-L, Olympus America Inc., Center Valley, PA, USA). Endothelial diameter (ED) was defined as the distance between external elastic laminae; vessels were categorised as small if ED was <50 µm and large if ED was >50 µm. Medial wall thickness (MWT) was determined as the distance between external and internal elastic laminae, calculated as a percentage using the following formula: $MWT=(2\times MT/ED)\times100$.

Immunofluorescence

See supplementary material for details.

ELISA

The levels of active TGF-β1, VEGF and ET-1 in rat and human bronchoalveolar lavage fluid (BALF) supernatants and sera were measured using a rat TGF-β1-specific ELISA kit (MB100B; R&D Systems), a rat VEGF ELISA kit (ab100786; Abcam), a rat ET-1 ELISA kit (E-EL-R0167; Elabscience, Houston, TX, USA) and a human ET-1 ELISA kit (DET100; R&D Systems) respectively, according to the manufacturer's recommendations.

Contraction assay

See supplementary material for details.

Statistical analysis

All data are expressed as median with interquartile range. Statistical analysis between two groups was performed using a non-parametric Mann–Whitney test. Statistical analysis between multiple groups with one control group was performed using a Kruskal–Wallis test, with a *post hoc* Dunn comparison. Analyses were performed with GraphPad Prism 6.0 (GraphPad Software Inc., La Jolla, CA, USA). A p-value <0.05 was considered significant.

Results

The ET-1 system is activated in IPF patients

Circulating ET-1 was measured in the sera of 31 IPF patients and nine aged-matched healthy controls. ET-1 was significantly upregulated in IPF (figure 1a). Circulating ET-1 correlated with predicted forced vital capacity (FVC) (figure 1b) and total lung capacity (TLC) (figure 1c). Expression of the ET receptor ETRA was upregulated in IPF patients compared to controls. The expression of ETRA was higher in advanced IPF than in moderate IPF (figure 1d, e). No difference between groups was found for the expression of ETRB (figure 1f, g).

Macitentan prevents PH induced by TGF-β1 in rats

Mean PAP significantly increased from D14 to D28 in AdTGF-β1 rats compared to controls (figure 2a). At D28, animals that received pirfenidone from D14 to D28 showed a non-significant decrease in mean PAP whereas macitentan normalised the increase in mean PAP induced by AdTGF-β1 (figure 2a).

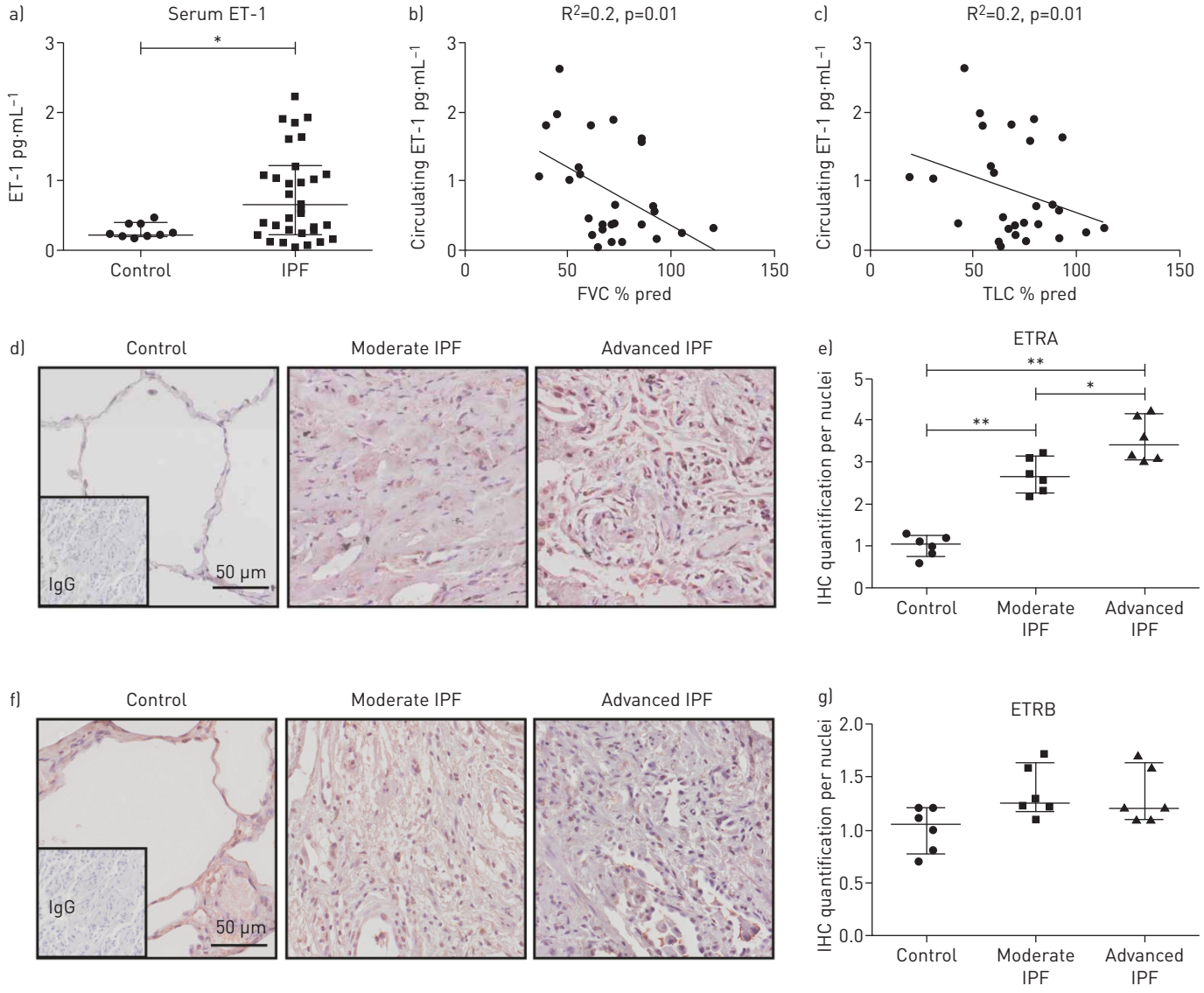

FIGURE 1 The ET-1 system is activated in idiopathic pulmonary fibrosis (IPF) patients. a) ET-1 protein level measured by ELISA in serum from healthy controls (n=9) and IPF patients (n=31); results are presented as median with interquartile range. *: p<0.05. b, c) Correlation between ET-1 level in sera of IPF patients and % predicted forced vital capacity (FVC) (b) and % predicted total lung capacity (TLC) (c). d) Representative images of immunohistochemistry (IHC) staining for ETRA made with the ImageJ software on tissue from control and IPF patients with moderate and advanced IPF. e) Quantification of IHC staining for ETRA; results are presented as median with interquartile range; n=6 per group. *: p<0.05, **: p<0.01. f) Representative images of IHC staining for ETRB made with ImageJ software on tissue from control and IPF patients with moderate and advanced IPF. g) Quantification of IHC staining for ETRB; results are presented as median with interquartile range; n=6 per group.

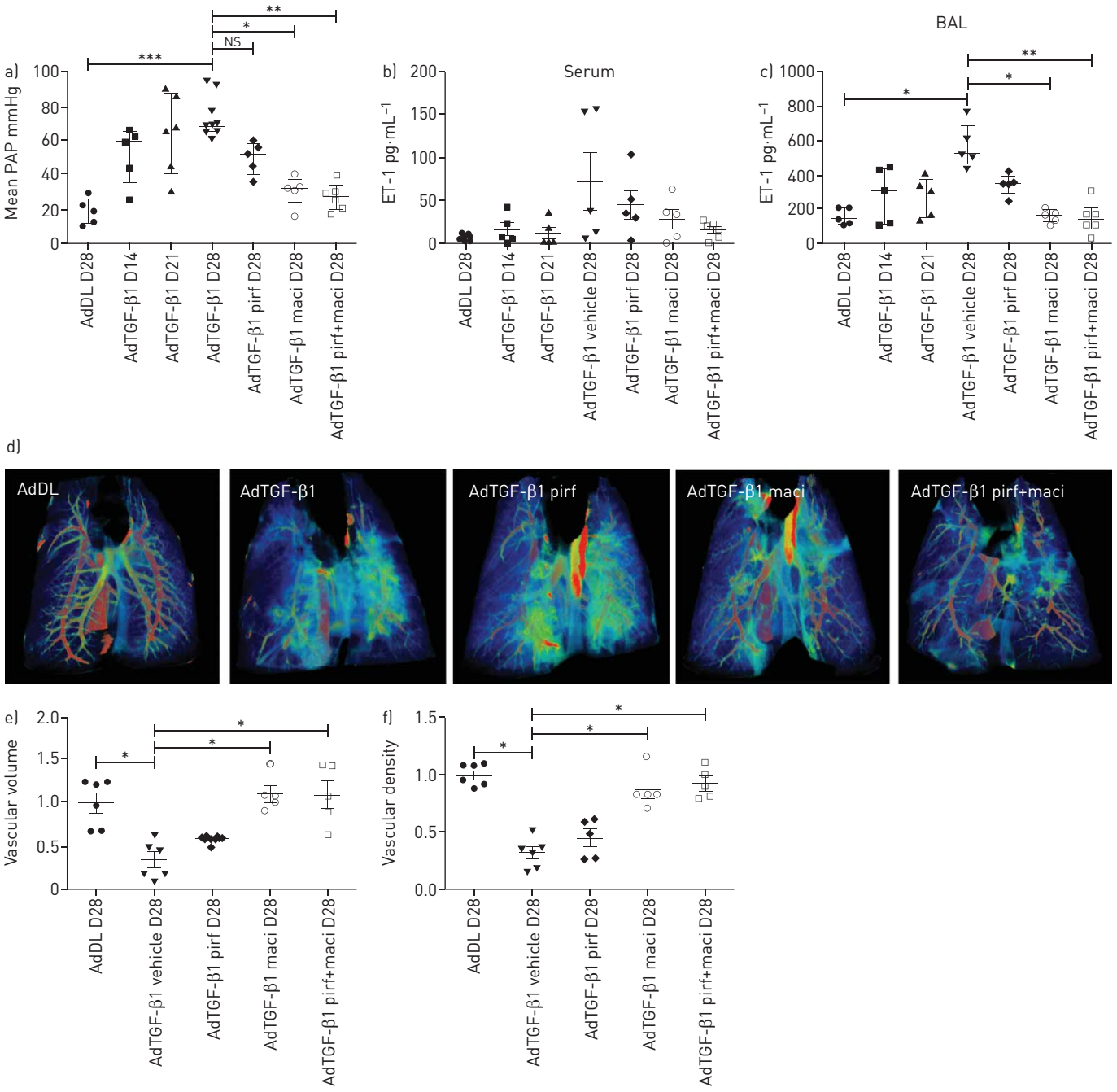

FIGURE 2 Macitentan (maci) but not pirfenidone (pirf) prevents pulmonary hypertension induced by TGF-β1. a) Mean pulmonary artery pressure (PAP) measured at time of death; data presented as median with interquartile range; n=5 for AdDL D28, AdTGF-β1 D14, AdTGF-β1 D21, AdTGF-β1 pirf D28 and AdTGF-β1 maci D28; n=6 for AdTGF-β1 pirf+maci D28; n=9 for AdTGF-β1 D28. NS: non-significant; *: p<0.05; **: p<0.01; ***: p<0.001. b, c) ET-1 protein level measured by ELISA in serum (b) and bronchoalveolar lavage (BAL) fluid (c); data presented as median with interquartile range; n=5 for AdDL D28, AdTGF-β1 D14, AdTGF-β1 D21, AdTGF-β1 D28, AdTGF-β1 pirf D28 and AdTGF-β1 maci D28; n=6 for AdTGF-β1 pirf+maci D28. *: p<0.05; **: p<0.01. d) Representative image of computed tomography (CT) scans of the vasculature of AdTGF-β1 (AdDL as control), AdTGF-β1 pirf, AdTGF-β1 maci and AdTGF-β1 pirf+maci rats at D28 obtained from AMIRA software. e) Vascular volume and f) vascular density calculated from CT scans of vasculature of AdTGF-β1 (AdDL as control), AdTGF-β1 pirf, AdTGF-β1 maci and AdTGF-β1 pirf+maci rats; data presented as mean±SEM; n=6 per group for AdDL and AdTGF-β1; n=5 per group for AdTGF-β1 pirf, AdTGF-β1 maci and AdTGF-β1 pirf+mac. *: p<0.05.

Animals that received the combination of macitentan and pirfenidone presented a similar mean PAP reduction to animals receiving macitentan alone (figure 2a).

The increase in mean PAP in AdTGF-β1 rats correlated with an increase in ET-1 in AdTGF-β1 rats compared to control in BALF but not in sera from D14 up to D28 (figure 2b, c). While pirfenidone had

no effect on ET-1, macitentan significantly reduced ET-1 in BALF when administered alone or in combination (figure 2c).

Computed tomography (CT) imaging allowed the quantification of vascular volume and density in large vessels (>75 μm) and demonstrated that AdTGF-β1 induced a decrease in lung vascular density and vascular volume, which was inhibited by macitentan alone or in combination; pirfenidone had no effect (figure 2d–f). In addition, the number of small (ED<50 μm) and large (ED>50 μm) pulmonary vessels at D28 in AdTGF-β1 animals was significantly reduced (supplementary figure S1A). Macitentan, but not pirfenidone, restored the number of both small and large vessels to levels comparable with controls. Vascular remodelling, assessed by MWT, was increased by D28 after AdTGF-β1 in small and large vessels (supplemental figure S1B, C). This increase in MWT was significantly reduced by macitentan and combination treatment (supplemental figure S1B, C).

Macitentan modulates VEGF expression in AdTGF-β1-treated rats

AdTGF-β1 induced an increase in VEGF in BALF but not serum at D28 (figure 3a, b). Macitentan significantly inhibited the VEGF increase induced by AdTGF-β1 in BALF but induced an increase in serum VEGF (figure 3a, b). Pirfenidone had no effect on VEGF (figure 3a, b). The effect of TGF-β1 on VEGF increase was confirmed in lung tissue from AdTGF-β1 rats at D28 (figure 3c, d); macitentan and combination therapy decreased VEGF expression, whereas pirfenidone had no effect (figure 3c, d). AdTGF-β1 induced a dramatic upregulation of VEGF expression in the parenchyma at D28 while no VEGF-positive ECs were found (figure 3e and supplementary figure S2). Macitentan alone or in combination reduced the expression of VEGF in the parenchyma while increasing VEGF in ECs (figure 3e and supplementary figure S2). Pirfenidone caused a similar expression of VEGF as AdTGF-β1 (figure 3e and supplementary figure S2). These results were confirmed on lung tissue by co-staining of CD31 and VEGF by immunofluorescence (supplementary figure S3A, B).

Macitentan and pirfenidone prevent the progression of AdTGF-β1-induced lung fibrosis

Hydroxyproline levels in AdTGF-β1 rats were increased compared to animals receiving the control adenovirus (AdDL) from D14 up to D28 (figure 4a). Macitentan, pirfenidone and their combination significantly lowered hydroxyproline content at D28 (figure 4a). AdTGF-β1 animals showed higher Ashcroft scores (figure 4b) than control. Ashcroft scores from animals receiving macitentan, pirfenidone and combination therapy were reduced compared to AdTGF-β1 (figure 4b). AdTGF-β1 rats had an increased fibrotic-area/whole-area ratio from D14 to D28 compared to control (quantitative assessment using ImageJ; figure 4c, d). Macitentan, pirfenidone and their combination reduced the percentage of fibrotic area compared to AdTGF-β1 (figure 4c, d). Picrosirius red staining was increased by AdTGF-β1 and was prevented by macitentan, pirfenidone and the combination therapy at D28 (figure 4e, f). Pressure–volume loop measurements at D28 demonstrated that both pirfenidone and macitentan induced an improvement in lung function compared with AdTGF-β1-treated rats (supplementary figure S4A). In addition, CT scanning allowed the area of fibrosis to be quantified in three-dimensional reconstructed lungs and demonstrated that macitentan and pirfenidone significantly reduced lung fibrosis induced by TGF-β1 (supplementary figure S4b).

Macitentan and pirfenidone inhibit pro-fibrotic pathways in vivo *in AdTGF-β1 rats*

At D28 endogenous total and active TGF-β1 was upregulated compared to controls (figure 5a, b). Treatment with macitentan, pirfenidone and their combination inhibited TGF-β1 upregulation. AdTGF-β1 induced upregulation of TGF-β1 at D28, which correlated with an increase in α-SMA (figure 5c, f). Smad3 phosphorylation, the main pathway of TGF-β1, was upregulated in AdTGF-β1 animals at D28 (figure 5c, d). Macitentan and, to a lesser extent, pirfenidone reduced AdTGF-β1-induced α-SMA and p-Smad3 upregulation (figure 5c, d, f). The combination of macitentan and pirfenidone had a comparable effect to macitentan alone (figure 5c–h). While AdTGF-β1 had no effect on ETRB, it significantly upregulated ETRA and ET-1 expression (figure 5c, e, g, h). Again, macitentan, pirfenidone and their combination inhibited both ETRA and ET-1 upregulation (figure 5c, g, h).

Mechanisms underlying the anti-fibrotic and anti-PH effects of macitentan

Macitentan blocked both ETRA and ETRB, which mediate ET-1 effects on VSMCs and ECs. *In vitro*, macitentan abolished VSMC contraction and EC death induced by recombinant ET-1 (rET-1) (supplementary figure S5A, B). Macitentan but not pirfenidone inhibited the contraction of lung fibroblasts induced by rET-1 and also by recombinant TGF-β1 (rTGF-β1) (figure 6a, b; supplementary figure S5a, b).

As expected, rTGF-β1 induced fibroblast-to-myofibroblast differentiation, as shown by the upregulation of collagen1, α-SMA and TGF-β1 mRNA (figure 6c–g). Interestingly, macitentan or pirfenidone alone

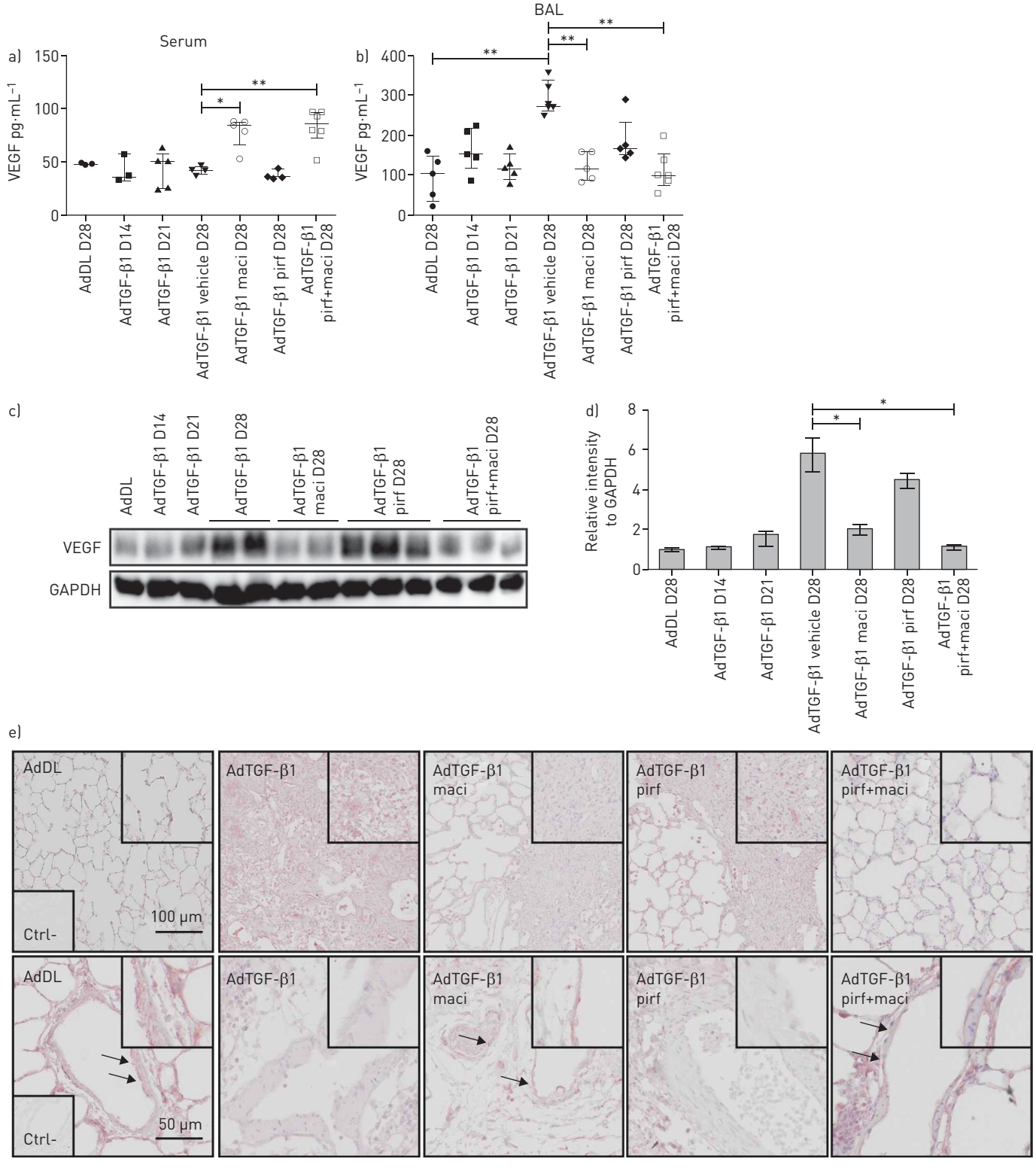

FIGURE 3 Macitentan (maci) but not pirfenidone (pirf) modulates VEGF expression in AdTGF-β1-treated rats. a, b) ET-1 protein level measured by ELISA in serum (a) and bronchoalveolar lavage (BAL) fluid (b); data presented as median with interquartile range; n=5 for AdDL D28, AdTGF-β1 D14, AdTGF-β1 D21, AdTGF-β1 D28, AdTGF-β1 maci D28 and AdTGF-β1 pirf D28; n=6 for AdTGF-β1 pirf+maci D28. *: p<0.05; **: p<0.01. c) VEGF expression measured by western blot in whole lung lysates of AdTGF-β1 (AdDL as control), AdTGF-β1 maci, AdTGF-β1 pirf and AdTGF-β1 pirf+maci rats. GAPDH was used as loading control. d) Relative intensity of VEGF expression was normalised with GAPDH using ImageJ; data are presented as median with interquartile range; n=4 per group. *: p<0.05. e) Representative images of immunohistochemistry of VEGF on AdTGF-β1 (AdDL as control), AdTGF-β1 maci, AdTGF-β1 pirf and AdTGF-β1 pirf+maci rats at D28. Upper row shows representative parenchymal area. Lower row shows representative vessels. Black arrows show VEGF-positive endothelial cells.

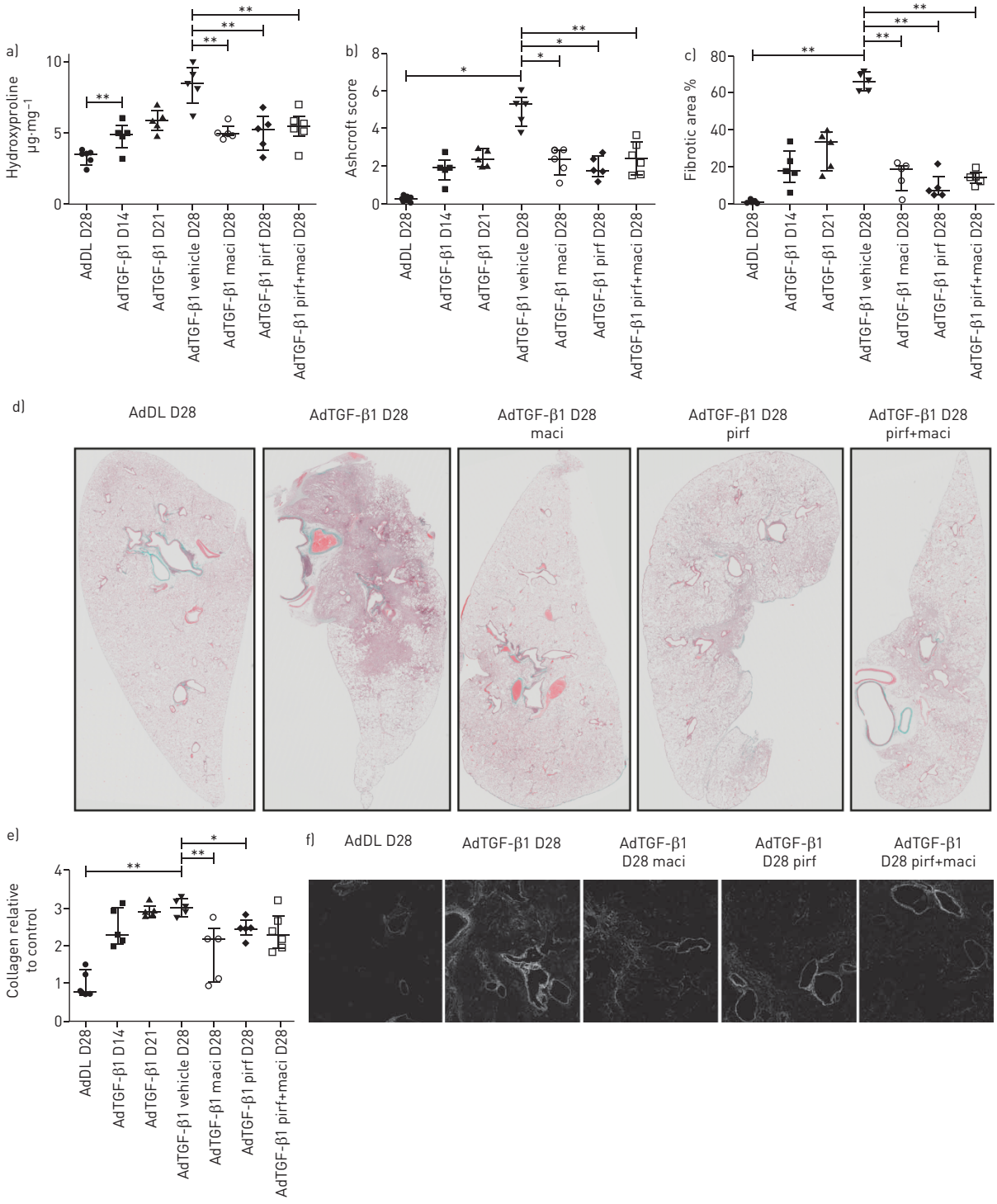

FIGURE 4 Macitentan (maci) and pirfenidone (pirf) prevent the progression of AdTGF-β1 induced lung fibrosis. a) Hydroxyproline measurements on whole lung lysates of AdTGF-β1 (AdDL as control), AdTGF-β1+maci, AdTGF-β1 pirf or AdTGF-β1 pirf+maci rats; data presented as median with interquartile range; n=5 for AdDL D28, AdTGF-β1 D14, AdTGF-β1 D21, AdTGF-β1 D28, AdTGF-β1 maci D28 and AdTGF-β1 pirf D28; n=6 for AdTGF-β1 pirf+maci D28. **: p<0.01. b) Ashcroft scoring and c) assessment of percentage of fibrotic area on lung sections stained by Masson trichrome from AdTGF-β1 (AdDL as control), AdTGF-β1 maci, AdTGF-β1 pirf and AdTGF-β1 pirf+maci rats; data presented as median with interquartile range; n=5 for AdDL D28, AdTGF-β1 D14, AdTGF-β1 D21, AdTGF-β1 D28, AdTGF-β1 maci D28 and AdTGF-β1 pirf D28; n=6 for AdTGF-β1 pirf+maci D28. *: p<0.05; **: p<0.01. d) Representative lung sections stained by Masson trichrome from AdTGF-β1 (AdDL as control), AdTGF-β1 maci, AdTGF-β1 pirf and AdTGF-β1 pirf+maci rats at D28 and imaged by slide scanner. e) Lung collagen quantification using Picrosirius (PSR) red intensity measurements on lung section from AdTGF-β1 (AdDL as control), AdTGF-β1 maci, AdTGF-β1 pirf and AdTGF-β1 pirf+maci rats; data are presented as median with interquartile range; n=5 for AdDL D28, AdTGF-β1 D14, AdTGF-β1 D21, AdTGF-β1 D28, AdTGF-β1 pirf D28 and AdTGF-β1 maci D28; n=6 for AdTGF-β1 pirf+maci D28. *: p<0.05; **: p<0.01. f) Representative lung sections stained by PSR from AdTGF-β1 (AdDL as control), AdTGF-β1 maci, AdTGF-β1 pirf and AdTGF-β1 pirf+maci rats at D28 and imaged by slide scanner.

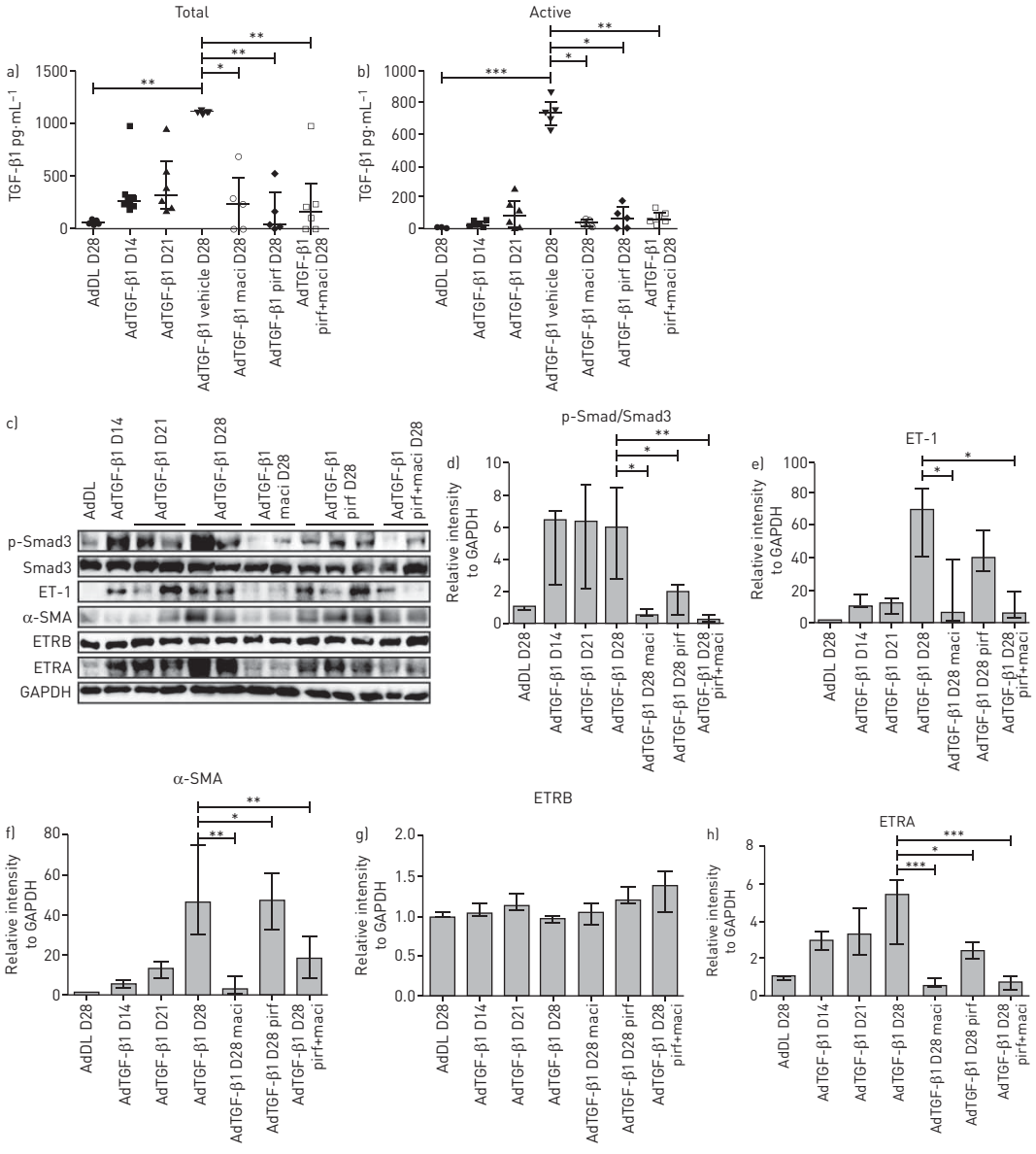

FIGURE 5 Macitentan (maci) and pirfenidone (pirf) inhibit pro-fibrotic pathways *in vivo* in AdTGF-β1 rats. a) Total and b) active TGF-β1 protein level measured by ELISA in bronchoalveolar lavage fluid of AdTGF-β1 (AdDL as control), AdTGF-β1 maci, AdTGF-β1 pirf and AdTGF-β1 pirf+maci rats; data presented as median with interquartile range; n=5 for AdDL D28, AdTGF-β1 D14, AdTGF-β1 D21, AdTGF-β1 D28, AdTGF-β1 maci D28 and AdTGF-β1 pirf D28; n=6 for AdTGF-β1 pirf+maci D28. *: p<0.05; **: p<0.01; ***: p<0.001. c) p-Smad3, Smad3, ET-1, α-SMA, ETRB and ETRA expression measured by western blot in whole lung lysates of AdTGF-β1 (AdDL as control), AdTGF-β1 maci, AdTGF-β1 pirf and AdTGF-β1 pirf +maci rats. GAPDH was used as loading control. d–h) Relative intensity of expression was normalised with GAPDH using ImageJ; data presented as median with interquartile range; n=6 per group. *: p<0.05; **: p<0.01; ***: p<0.001.

inhibited this upregulation (figure 6c–g). The combination of macitentan and pirfenidone showed even lower levels of mRNA for collagen1, α-SMA and TGF-β1 (figure 6c–g). The mRNA findings were confirmed at the protein level (figure 6c–g). VEGF and TGF-β1 expression were enhanced in fibroblasts by rTGF-β1 and inhibited by macitentan and pirfenidone (figure 6c–g). In addition, active caspase-3 expression was reduced in fibroblasts that received rTGF-β1 and active caspase-3 levels were restored by macitentan and pirfenidone (figure 6c–g). Collagen1A protein expression was strongly reduced by macitentan but not pirfenidone.

Similarly, rTGF-β1 induced mRNA upregulation of collagen1A, α-SMA and TGF-β1 in ECs, suggesting differentiation of EC into myofibroblast-like cells (figure 6h–l). Macitentan alone and in combination with pirfenidone inhibited collagen1A, α-SMA and TGF-β1 mRNA upregulation whereas pirfenidone alone had no effect (figure 6h–l). Interestingly, VEGF mRNA expression was strongly upregulated by macitentan

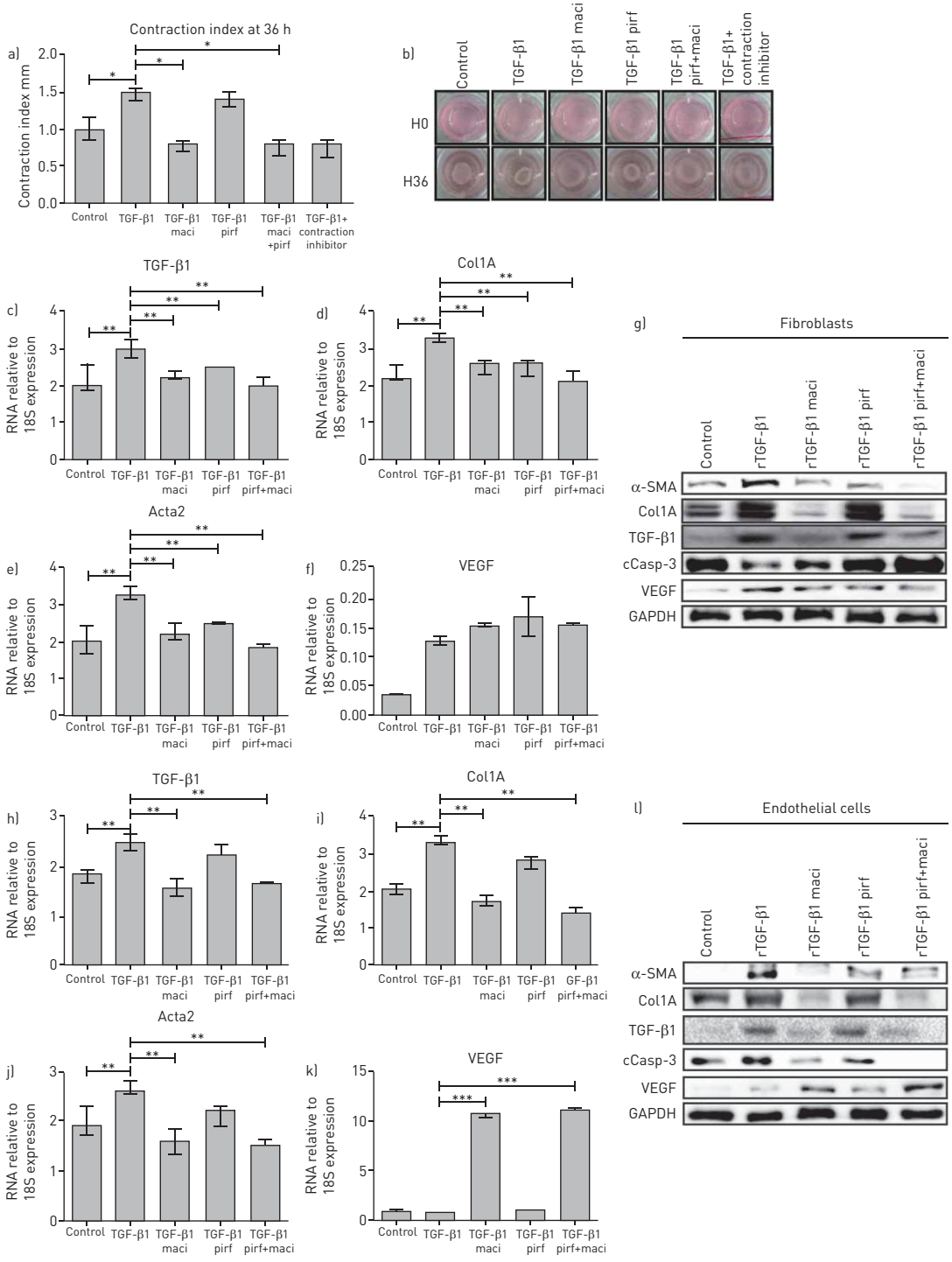

FIGURE 6 Macitentan (maci) induces myofibroblast apoptosis and protects endothelial cells *in vitro*. a) Control human fibroblasts mixed in a collagen gel cultured in 24-well plates for 12 h in medium without fetal bovine serum. After 12 h cells are treated with TGF-β1 (5 ng·mL^{-1}) and maci (100 µM), pirfenidone (pirf; 100 µM) or a combination for 24 h. After 24 h gels were released for the edge of each well and gel contraction was measured every 2 h. Graphs show contraction index (mm) at 36 h and evolution of contraction from 0 to 36 h after gel release; data are presented as median with interquartile range; n=5. *: p<0.05. b) Representative gel contraction at 0 h and 36 h. c–f) mRNA expression of TGF-β1 (c), Collagen1A (Col1A) (d), Acta2 (e) and VEGF (f) in human control fibroblasts 24 h after treatment with rTGF-β1 (5 ng·mL^{-1}) and maci (100 µM), pirf (100 µM) or a combination; data presented as median with interquartile range; n=6. **: p<0.01. g) Expression of α-SMA, TGF-β1, Col1A, cleaved caspase-3 (cCasp-3) and VEGF in human control fibroblasts analysed by western blot 48 h after treatment with rTGF-β1 (5 ng·mL^{-1}) and maci (100 µM), pirf (100 µM) or a combination. GAPDH was used as loading control. h–k) mRNA expression of TGF-β1, Col1A, VEGF and Acta2 in human pulmonary artery endothelial cells 24 h after treatment with rTGF-β1 (5 ng·mL^{-1}) and maci (100 µM), pirf (100 µM) or a combination; data presented as median with interquartile range; n=6. **: p<0.01; ***: p<0.001. l) Expression of α-SMA, Col1A, TGF-β1, cCasp-3 and VEGF in human pulmonary artery endothelial cells analysed by western blot 48 h after treatment with rTGF-β1 (5 ng·mL^{-1}) and maci (100 µM), pirf (100 µM) or a combination. GAPDH was used as loading control.

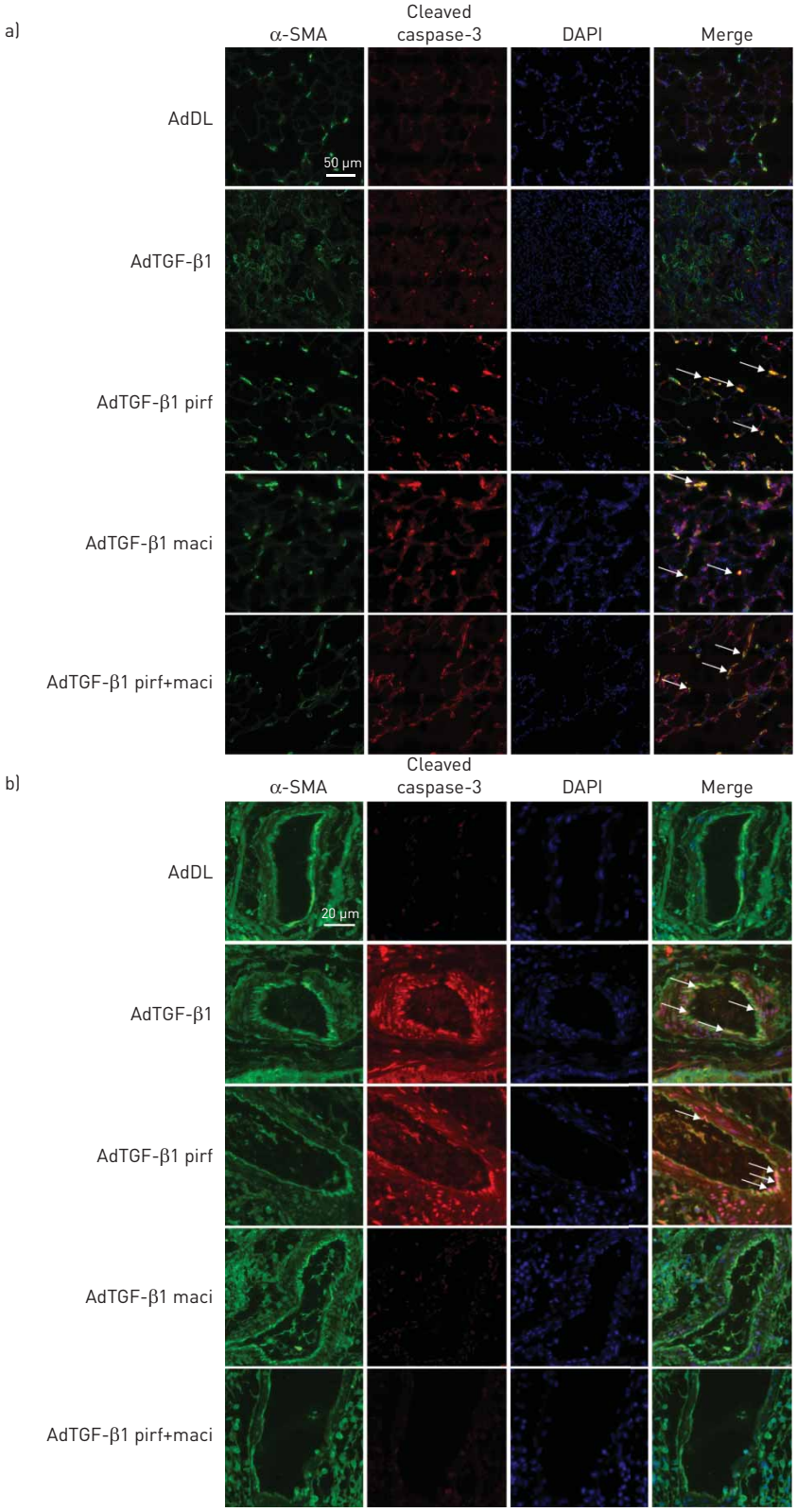

FIGURE 7 Macitentan (maci) induces myofibroblast apoptosis and protects endothelial cells *in vivo*. a) Representative images of dual immunofluorescent staining of α-SMA (green) and cleaved caspase-3 (red) on lung sections from rats treated with AdTGF-β1 (AdDL as control), AdTGF-β1 pirfenidone (pirf), AdTGF-β1 maci and AdTGF-β1 pirf+maci at D28. DAPI was used a nuclear marker. White arrows show α-SMA+/caspase-3+ cells. b) Representative image of dual immunofluorescent staining of CD31 (green) and cleaved caspase-3 (red) on lung sections from rats treated with AdTGF-β1 (AdDL as control), AdTGF-β1 pirf, AdTGF-β1 maci and AdTGF-β1 pirf+maci at D28. DAPI was used a nuclear marker. White arrows show CD31+/caspase-3+ cells.

but not pirfenidone (figure 6h–l). At the protein level, α-SMA expression in ECs was upregulated by rTGF-β1 and inhibited by macitentan and, to a lesser extent, pirfenidone (figure 6h–l). VEGF and active caspase-3 regulation in ECs was opposite to that in fibroblasts. In EC, rTGF-β1 induced an increase in caspase-3 and a decrease in VEGF (figure 6h–l) whereas macitentan, but not pirfenidone, restored VEGF and inhibited caspase-3 expression induced by rTGF-β1 (figure 6h–l). Our results demonstrate that, along with EC apoptosis, ET-1 induced the secretion of latent TGF-β1 and its activation (supplementary figure S5C). Macitentan alone and in combination with pirfenidone inhibited TGF-β1 secretion and activation whereas pirfenidone alone had no effect (supplementary figure S5C).

In vivo, AdTGF-β1 induced only a few caspase-3-positive cells in the parenchyma (fibroblasts) but significant EC apoptosis (supplementary figure S6). Pirfenidone-treated rats had high numbers of caspase-3-positive cells both in parenchyma and endothelium. By contrast, macitentan alone and combination therapy increased caspase-3-positive cells only in the parenchyma while protecting ECs from apoptosis (supplementary figure S6). Dual fluorescent staining confirmed that macitentan, pirfenidone and their combination increased caspase-3-positive/α-SMA-positive cells, indicating an increase in myofibroblast apoptosis compared to AdTGF-β1 (figure 7a). In contrast, AdTGF-β1 induced an increase in caspase-3-positive/CD31-positive cells, indicating increased EC apoptosis. Macitentan and the combination therapy but not pirfenidone alone reduced AdTGF-β1-induced EC apoptosis (figure 7b).

Discussion

IPF is a progressive disease with poor prognosis and limited therapeutic options. To date only two drugs, nintedanib and pirfenidone [1, 2], affect disease progression; these were recently approved for the treatment of IPF. PH is a frequent complication of IPF with an incidence of 32–73% [15]. The development of PH in IPF is associated with poor prognosis and increased hospitalisation. PH usually develops at advanced stages of IPF; thus, managing PH becomes a valid option to improve patient outcome.

In the current study we show that pulmonary fibrosis mediated by the overexpression of active TGF-β1 induces significant PH. Along with an increase in ECM deposition, vascular remodelling was observed in AdTGF-β1 rats with rarefaction of the vasculature, increased vessel wall thickness and EC apoptosis, leading to increased mean PAP. Macitentan, a dual endothelin receptor antagonist approved for the treatment of PAH, prevents vascular remodelling and PAH in various animal models [11, 16, 17]. As expected, in our model, macitentan counteracted the development of PH induced by AdTGF-β1 as shown by a reduced mean PAP. This improvement was associated with an increase in vascular density. Macitentan prevented EC apoptosis promoting the production of VEGF, which may be involved in vasculature rarefaction. In contrast, pirfenidone showed only moderate effects on PH, suggesting a specific effect of macitentan on the vasculature.

In addition, we demonstrate in this study that therapeutic administration of macitentan in fibrotic lungs prevents fibrosis progression. Pirfenidone is an established anti-fibrotic drug that inhibits experimental lung fibrosis [18–20]. The anti-fibrotic efficacy of macitentan was identical to that of pirfenidone in our model. By D28, collagen deposition in rats receiving macitentan or pirfenidone was reduced compared to that in rats receiving AdTGF-β1 and no drug. Collagen levels in AdTGF-β1 plus macitentan or AdTGF-β1 plus pirfenidone rats at D28 were comparable with the level in AdTGF-β1 rats by D14, suggesting that macitentan and pirfenidone prevented further collagen deposition from D14 to D28 rather than reducing existing fibrosis. The combination of pirfenidone and macitentan did not provide any additional beneficial effect on fibrosis progression compared to monotherapy.

The current paradigm for IPF pathobiology suggests that epithelial micro-injuries of unknown aetiology lead to an increase in pro-fibrotic mediators, such as active TGF-β1, which create a pro-fibrotic microenvironment in the lung. The differentiation of fibroblasts into myofibroblasts with the formation of fibroblast foci is a central step promoting the production of ECM responsible for the disruption of the alveolar architecture [21]. Unlike epithelial/endothelial cells, IPF myofibroblasts are resistant to apoptosis [22]. Pirfenidone inhibits fibroblast-to-myofibroblast differentiation and ECM production and reduces myofibroblast proliferation *in vitro* and *in vivo* [23, 24]. Our findings confirm that pirfenidone exerts anti-fibrotic effects, including inhibiting α-SMA expression in myofibroblasts, TGF-β1 expression and collagen deposition induced by TGF-β1 *in vitro* in fibroblasts and by reducing the pool of myofibroblasts *in vivo* through promoting apoptosis.

It has been demonstrated that ET receptor antagonists ameliorate bleomycin-induced pulmonary fibrosis [8]. Moreover, in a model of systemic sclerosis (SSc), macitentan inhibited the pro-fibrotic myofibroblast phenotype induced by ET-1 in human skin fibroblasts [25]. Circulating or tissue ET-1 levels are upregulated in IPF and SSc patients and in the bleomycin model of pulmonary fibrosis [26–28]. We demonstrate here that macitentan, like pirfenidone, prevents TGF-β1-induced myofibroblast differentiation

in vitro and induces myofibroblast apoptosis *in vivo*. In our model, both TGF-β1 and ET-1 were upregulated until D28. Whereas macitentan reduced both TGF-β1 and ET-1 levels, pirfenidone inhibited only TGF-β1, suggesting a specific action of macitentan on the ET-1 system. This explains the added benefit of the combination of both drugs on inhibiting fibroblast differentiation *in vitro*. Cipriani *et al.* [29] demonstrated the formation of an ET-1/TGF-β receptor complex in fibroblasts from SSc patients, which highlighted potential interference between ET receptor and TGF-β signalling. Therefore, it is not surprising that macitentan, by blocking ET-1 signalling, also inhibits TGF-β1.

The differentiation of ECs into myofibroblasts, called endothelial-to-mesenchymal transition (endoMT), is one of the putative sources for myofibroblasts in fibrosis [30]. We have demonstrated that, in addition to its effect on fibroblast differentiation, macitentan but not pirfenidone inhibits EC differentiation *in vitro* and prevents EC death *in vivo*. EndoMT has also been implicated in the pathogenesis of idiopathic PAH and SSc-PH [31, 32], by promoting vascular remodelling and vasoconstriction. Thus, by inhibiting endoMT and protecting ECs from apoptosis, macitentan protects AdTGF-β1 rats from PH and may protect AdTGF-β1 rats from subsequent fibrosis, whereas pirfenidone only acts on fibrosis progression. Nevertheless, while endoMT has been demonstrated to promote lung fibrosis in animal models, the exact contribution of endoMT in human IPF remains elusive and the exact role of macitentan on EC differentiation in IPF requires further investigation. It has been demonstrated that EC death induces latent TGF-β1 release in the extracellular compartment and stimulates its activation [33]. In our model, macitentan prevented TGF-β1 release and activation from ECs, thus limiting AdTGF-β1-induced fibrosis progression.

VEGF is an important contributing factor to both PAH and fibrosis. We have previously demonstrated that VEGF reduces apoptosis of ECs and vascular rarefaction, thereby improving PH [10]. However, augmentation of VEGF expression can also worsen fibrosis [10]. It has been shown that macitentan inhibits VEGF in a model of type 2 diabetes [34]. In our study, VEGF expression in whole lungs was upregulated following AdTGF-β1, confirming a putative pro-fibrotic effect of VEGF. VEGF was dramatically reduced by macitentan but not pirfenidone. Still, the reduction of VEGF expression seems to conflict with the vascular protection provided by macitentan. VEGF is a potent cytokine and only a little localised presence of VEGF may prove sufficient to exert its angiogenetic properties. Interestingly, after AdTGF-β1 the expression of VEGF was largely increased in the lung parenchyma whereas it was inhibited around ECs. In contrast, macitentan abolished parenchymal VEGF expression while enhancing its expression in the endothelial layer, which is noteworthy considering that VEGF is an important survival signal for ECs.

We demonstrate here that pirfenidone exerts its anti-fibrotic action by reducing ECM/TGF-β1 production, mainly by inhibiting fibroblast-to-myofibroblast differentiation and promoting myofibroblast apoptosis. In contrast, the anti-fibrotic capacity of macitentan is not limited by its action on fibroblasts.

Our study also confirms previous results showing that circulating ET-1 is upregulated in IPF patients [35], along with ETRA. Moreover, we were able to demonstrate a correlation between IPF severity and ET-1 serum level. This supports a potential role for ET-1 blockers in advanced IPF, but these findings need to be confirmed. We strongly believe that this argument holds true even when considering that the MUSIC trial reported that macitentan was not effective for the treatment of IPF [12]. In our preclinical model, lung fibrosis was correlated with vascular remodelling including EC death and PH. Signals sent by EC damage, such as latent TGF-β1 release and activation, likely worsen fibrosis, a process inhibited by macitentan in rats. While results obtained in preclinical models are certainly not always transposable to humans, we believe that our AdTGF-β1 model may be representative of a population of IPF patients with lung fibrosis and PH that has not specifically been investigated in previous clinical trials. The MUSIC trial, just like an earlier trial investigating the effect of bosentan, another ETRA/ETRB antagonist, was conducted in patients with mild to moderate IPF who probably did not (yet) have significant remodelling of the pulmonary vasculature and PH [36, 37]. The more recent ARTEMIS trial concluded that ambrisentan, an antagonist selective for ETRA, was not effective in treating IPF and may even be associated with an increased risk for disease progression [38]. Still, ARTEMIS was terminated early, which means that exposure to the drug may not have been long enough to see a benefit and only a small fraction of study subjects had group 3 PH (14%) [39]. It is likely that macitentan may have beneficial effects only in a restricted population of IPF patients with advanced disease and PH development, which may not have been highlighted in previous clinical trials.

In summary, we demonstrate a solid anti-fibrotic effect of macitentan on pulmonary fibrosis in a non-inflammation-driven experimental model of lung fibrosis. The effect is similar to that of pirfenidone, one of the two approved anti-fibrotic drugs. In addition, macitentan, alone and in combination with pirfenidone, significantly improved PH and reduced pulmonary vessel remodelling in animals with advanced fibrosis plus PH. These findings strongly support what the investigators of the ARTEMIS trials

have postulated in their summarising statement [39]: "*The observations in this limited number of patients with WHO [World Health Organization] group 3 PH warrant further studies to understand the pathophysiogical aspects and clinical outcomes of the pulmonary vasculopathy associated with IPF.*"

Acknowledgements: The authors thank Fuqin Duan for her excellent technical help. We thank Jennifer Wattie and Rod Rhem for their help with the rodent CT scan experiments. We thank Anna Dvorkin-Gheva for her efficient technical help with the Nanostring analysis.

Conflict of interest: M. Iglarz is an employee of Actelion Pharmaceuticals Ltd, the manufacturer of macitentan. M. Kolb reports grants and personal fees from Roche, Boehringer Ingelheim, GSK, Gilead, Prometic and Alkermes, grants from Actelion, Respivert and Synairgen, and personal fees from AstraZeneca and Genoa, outside the submitted work.

Support statement: Funding for this study was granted by Actelion Pharmaceuticals Ltd. P-S. Bellaye is funded by le Fonds de Dotation "Recherche en Santé Respiratoire et de la Fondation du Souffle", the Canadian Pulmonary Fibrosis Foundation (CPFF) and the Research Institute of St Joseph's Hospital, Hamilton, ON, Canada (FSORC Award). C. Shimbori is funded by the Pulmonary Fibrosis Foundation (I.M. Rosenzweig Junior Investigator Award) and Mitacs Canada. Funding information for this article has been deposited with the Crossref Funder Registry.

References

1 King TE Jr, Bradford WZ, Castro-Bernardini S, *et al.* A phase 3 trial of pirfenidone in patients with idiopathic pulmonary fibrosis. *N Engl J Med* 2014; 370: 2083–2092.
2 Richeldi L, du Bois RM, Raghu G, *et al.* Efficacy and safety of nintedanib in idiopathic pulmonary fibrosis. *N Engl J Med* 2014; 370: 2071–2082.
3 Raghu G. Idiopathic pulmonary fibrosis: lessons from clinical trials over the past 25 years. *Eur Respir J* 2017; 50: 1701209.
4 Blobe GC, Schiemann WP, Lodish HF. Role of transforming growth factor beta in human disease. *N Engl J Med* 2000; 342: 1350–1358.
5 Patel NM, Lederer DJ, Borczuk AC, *et al.* Pulmonary hypertension in idiopathic pulmonary fibrosis. *Chest* 2007; 132: 998–1006.
6 Pulido T, Adzerikho I, Channick RN, *et al.* Macitentan and morbidity and mortality in pulmonary arterial hypertension. *N Engl J Med* 2013; 369: 809–818.
7 Elisa T, Antonio P, Giuseppe P, *et al.* Endothelin receptors expressed by immune cells are involved in modulation of inflammation and in fibrosis: relevance to the pathogenesis of systemic sclerosis. *J Immunol Res* 2015; 2015: 147616.
8 Park SH, Saleh D, Giaid A, *et al.* Increased endothelin-1 in bleomycin-induced pulmonary fibrosis and the effect of an endothelin receptor antagonist. *Am J Respir Crit Care Med* 1997; 156: 600–608.
9 Shi-Wen X, Chen Y, Denton CP, *et al.* Endothelin-1 promotes myofibroblast induction through the ETA receptor via a rac/phosphoinositide 3-kinase/Akt-dependent pathway and is essential for the enhanced contractile phenotype of fibrotic fibroblasts. *Mol Biol Cell* 2004; 15: 2707–2719.
10 Farkas L, Farkas D, Ask K, *et al.* VEGF ameliorates pulmonary hypertension through inhibition of endothelial apoptosis in experimental lung fibrosis in rats. *J Clin Invest* 2009; 119: 1298–1311.
11 Iglarz M, Steiner P, Wanner D, *et al.* Vascular effects of endothelin receptor antagonists depends on their selectivity for ETA *versus* ETB receptors and on the functionality of endothelial ETB receptors. *J Cardiovasc Pharmacol* 2015; 66: 332–337.
12 Raghu G, Million-Rousseau R, Morganti A, *et al.* Macitentan for the treatment of idiopathic pulmonary fibrosis: the randomised controlled MUSIC trial. *Eur Respir J* 2013; 42: 1622–1632.
13 Ask K, Bonniaud P, Maass K, *et al.* Progressive pulmonary fibrosis is mediated by TGF-beta isoform 1 but not TGF-beta3. *Int J Biochem Cell Biol* 2008; 40: 484–495.
14 Hubner RH, Gitter W, El Mokhtari NE, *et al.* Standardized quantification of pulmonary fibrosis in histological samples. *BioTechniques* 2008: 44: 507–511, 514–507.
15 Shorr AF, Wainright JL, Cors CS, *et al.* Pulmonary hypertension in patients with pulmonary fibrosis awaiting lung transplant. *Eur Respir J* 2007; 30: 715–721.
16 Temple IP, Monfredi O, Quigley G, *et al.* Macitentan treatment retards the progression of established pulmonary arterial hypertension in an animal model. *Int J Cardiol* 2014; 177: 423–428.
17 Iglarz M, Landskroner K, Bauer Y, *et al.* Comparison of macitentan and bosentan on right ventricular remodeling in a rat model of non-vasoreactive pulmonary hypertension. *J Cardiovasc Pharmacol* 2015; 66: 457–467.
18 Inomata M, Kamio K, Azuma A, *et al.* Pirfenidone inhibits fibrocyte accumulation in the lungs in bleomycin-induced murine pulmonary fibrosis. *Respir Res* 2014; 15: 16.
19 Kakugawa T, Mukae H, Hayashi T, *et al.* Pirfenidone attenuates expression of HSP47 in murine bleomycin-induced pulmonary fibrosis. *Eur Respir J* 2004; 24: 57–65.
20 Antoniu SA. Pirfenidone for the treatment of idiopathic pulmonary fibrosis. *Expert Opin Investig Drugs* 2006; 15: 823–828.
21 Barkauskas CE, Noble PW. Cellular mechanisms of tissue fibrosis. 7. New insights into the cellular mechanisms of pulmonary fibrosis. *Am J Physiol Cell Physiol* 2014; 306: C987–C996.
22 Thannickal VJ, Horowitz JC. Evolving concepts of apoptosis in idiopathic pulmonary fibrosis. *Proc Am Thorac Soc* 2006; 3: 350–356.
23 Shin JM, Park JH, Park IH, *et al.* Pirfenidone inhibits transforming growth factor beta1-induced extracellular matrix production in nasal polyp-derived fibroblasts. *Am J Rhinol Allergy* 2015; 29: 408–413.
24 Lehtonen ST, Veijola A, Karvonen H, *et al.* Pirfenidone and nintedanib modulate properties of fibroblasts and myofibroblasts in idiopathic pulmonary fibrosis. *Respir Res* 2016; 17: 14.
25 Cutolo M, Montagna P, Brizzolara R, *et al.* Effects of macitentan and its active metabolite on cultured human systemic sclerosis and control skin fibroblasts. *J Rheumatol* 2015; 42: 456–463.

26 Cambrey AD, Harrison NK, Dawes KE, *et al.* Increased levels of endothelin-1 in bronchoalveolar lavage fluid from patients with systemic sclerosis contribute to fibroblast mitogenic activity in vitro. *Am J Respir Cell Mol Biol* 1994; 11: 439–445.
27 Uguccioni M, Pulsatelli L, Grigolo B, *et al.* Endothelin-1 in idiopathic pulmonary fibrosis. *J Clin Pathol* 1995; 48: 330–334.
28 Mutsaers SE, Foster ML, Chambers RC, *et al.* Increased endothelin-1 and its localization during the development of bleomycin-induced pulmonary fibrosis in rats. *Am J Respir Cell Mol Biol* 1998; 18: 611–619.
29 Cipriani P, Di Benedetto P, Ruscitti P, *et al.* Macitentan inhibits the transforming growth factor-beta profibrotic action, blocking the signaling mediated by the ETR/TbetaRI complex in systemic sclerosis dermal fibroblasts. *Arthritis Res Ther* 2015; 17: 247.
30 Piera-Velazquez S, Mendoza FA, Jimenez SA. Endothelial to mesenchymal transition (EndoMT) in the pathogenesis of human fibrotic diseases. *J Clin Med* 2016; 5: E45.
31 Good RB, Gilbane AJ, Trinder SL, *et al.* Endothelial to Mesenchymal transition contributes to endothelial dysfunction in pulmonary arterial hypertension. *Am J Pathol* 2015; 185: 1850–1858.
32 Ranchoux B, Antigny F, Rucker-Martin C, *et al.* Endothelial-to-mesenchymal transition in pulmonary hypertension. *Circulation* 2015; 131: 1006–1018.
33 Sakao S, Taraseviciene-Stewart L, Wood K, *et al.* Apoptosis of pulmonary microvascular endothelial cells stimulates vascular smooth muscle cell growth. *Am J Physiol Lung Cell Mol Physiol* 2006; 291: L362–L368.
34 Sen S, Chen S, Feng B, *et al.* Renal, retinal and cardiac changes in type 2 diabetes are attenuated by macitentan, a dual endothelin receptor antagonist. *Life Sci* 2012; 91: 658–668.
35 Barlo NP, van Moorsel CH, Kazemier KM, *et al.* Potential role of endothelin-1 in pulmonary fibrosis: from the bench to the clinic. *Am J Respir Cell Mol Biol* 2010; 42: 633.
36 King TE Jr, Behr J, Brown KK, *et al.* BUILD-1: a randomized placebo-controlled trial of bosentan in idiopathic pulmonary fibrosis. *Am J Respir Crit Care Med* 2008; 177: 75–81.
37 King TE Jr, Brown KK, Raghu G, *et al.* BUILD-3: a randomized, controlled trial of bosentan in idiopathic pulmonary fibrosis. *Am J Respir Crit Care Med* 2011; 184: 92–99.
38 Raghu G, Behr J, Brown KK, *et al.* Treatment of idiopathic pulmonary fibrosis with ambrisentan: a parallel, randomized trial. *Ann Intern Med* 2013; 158: 641–649.
39 Raghu G, Nathan SD, Behr J, *et al.* Pulmonary hypertension in idiopathic pulmonary fibrosis with mild-to-moderate restriction. *Eur Respir J* 2015; 46: 1370–1377.